The Astrophysical Journal, 585:298–304, 2003 March 1

CHANDRA STUDIES OF THE X-RAY POINT SOURCE LUMINOSITY FUNCTIONS OF M31

Albert K. H. Kong
Harvard-Smithsonian Center for Astrophysics, 60 Garden Street, Cambridge, MA 02138

Rosanne DiStefano
Harvard-Smithsonian Center for Astrophysics, 60 Garden Street, Cambridge, MA 02138; and Department of Physics and Astronomy, Tufts University, Medford, MA 02155

Michael R. Garcia
Harvard-Smithsonian Center for Astrophysics, 60 Garden Street, Cambridge, MA 02138

and

Jochen Greiner
Max-Plank-Institut für extraterrestrische Physik, Postfach 1603, 85740 Garching, Germany
Received 2002 July 11; accepted 2002 November 5

ABSTRACT

Three different M31 disk fields, spanning a range of stellar populations, were observed by *Chandra*. We report the X-ray point source luminosity function (LF) of each region, and the LF of M31's globular clusters, and compare these with each other and with the LF of the galaxy's bulge. To interpret the results we also consider tracers of the stellar population, such as OB associations and supernova remnants. We find differences in the LFs among the fields, but cannot definitively relate them to the stellar content of the fields. We find that stellar population information, average and maximum source luminosities, X-ray source densities, and slopes of the LF are useful in combination.

Subject headings: galaxies: individual (M31) — X-rays: binaries — X-rays: galaxies

1. INTRODUCTION

The luminosity function (LF) of point X-ray sources can provide useful information about galactic stellar populations. *Chandra*'s good angular resolution allows detailed X-ray source population studies of external galaxies. Because M31 is close (780 kpc; Stanek & Garnavich 1998; Macri et al. 2001), we can probe its LF to luminosities as low as a few times 10^{35} ergs s^{-1} with ~15–45 ks *Chandra* exposures. M31 is therefore an excellent extragalactic spiral galaxy in which to study X-ray source populations with a wide range of luminosities. Previous studies of M31's LF (*Einstein*, Trinchieri & Fabbiano 1991; *ROSAT*, Primini, Forman, & Jones 1993, Supper et al. 1997; *XMM-Newton*, Shirey et al. 2001; and *Chandra*, Kong et al. 2002b; Kaaret 2002) have concentrated on the central region ($<30'$). In particular, Kong et al. (2002b) found that the shape of the LF varies with radius even in the central $17' \times 17'$ region. More recently, Trudolyubov et al. (2002) used *XMM-Newton* to study the LF of the northern disk and found it to differ from that of the central region, suggesting a different source population.

In this paper, we present the LFs of three M31 disk regions as observed by *Chandra*. We compare them to LFs of the central region (Kong et al. 2002b) and of globular clusters (GCs; Di Stefano et al. 2002). We find that the slopes of the LFs are of limited use in relating X-ray source populations to stellar populations. We therefore include in our study other quantities derived from the X-ray data (e.g., source densities, and average and maximum luminosities) as well as optical tracers of the stellar population.

2. OBSERVATIONS AND DATA REDUCTION

Figure 1 shows the fields of view of the *Chandra* ACIS-S[1] observations of M31. Three disk regions of M31 were chosen to span a wide range of M31 stellar populations; each was observed three times (~15 ks for each ACIS-S observation) at intervals of 3–4 months during 2000–2001 (PI: Di Stefano). A detailed description of the observations will be presented in a companion paper.

Field 1, centered at R.A. $= 00^h38^m37^s$, decl. $= +40°17'41''$, is farthest from the galaxy center. Field 3 is closer to the galaxy center, but the aim point (R.A. $= 00^h46^m17^s$, decl. $= +41°41'07''$) is offset from the long axis of M31's disk. Those parts of field 3 closest to the central axis encompass an arc of M31's 10 kpc star-forming ring (e.g., Haas et al. 1998). Because the portion of field 3 away from the ring contains an apparently distinct, older, stellar population, we have divided field 3 into two distinct parts: field 3A includes the star-forming ring (X-ray sources in field 3A are shown in red), while field 3B is the largest portion of the field and does not include the ring. Field 2 is close to the center of the galaxy (R.A. $= 00^h41^m53^s$, decl. $= +41°00'45''$). Part of it overlaps the bulge and the central $17' \times 17'$ region that has been studied with *Chandra* ACIS-I (Kong et al. 2002b; Fig. 1, *red polygon*). Because the part of this region closest to the nucleus is far off axis ($>15'$) in a crowded field, we consider it separately, calling it field 2B

[1] Details about ACIS can be found at http://asc.harvard.edu/udocs/docs/POG/MPOG/node11.html.

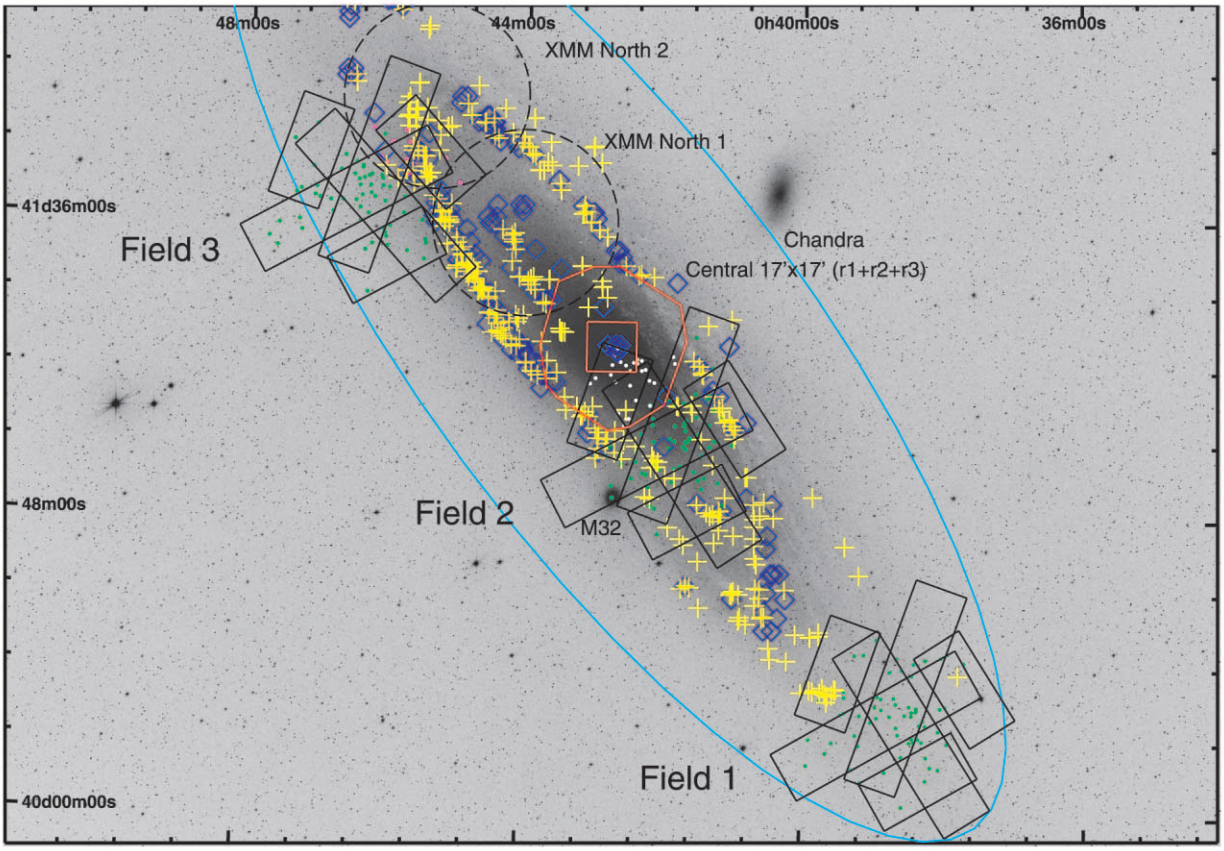

FIG. 1.—Regions observed by *Chandra* ACIS-S and the detected X-ray sources: fields 1, 2A, and 3B (*green dots*), field 2B (*white dots*), and field 3A (*red dots*) overlaid on an optical Digital Sky Survey image of M31. The fields of view of the two *XMM-Newton* observations (*dashed circles*) and *Chandra* ACIS-I observations (*red polygon*) of the central region (Kong et al. 2002b) are also shown; the central red square inside the polygon is the central $8' \times 8'$ region ($r1 + r2$ in Kong et al. 2002b). The asymmetric shape of the ACIS-I region is due to combining observations with different roll angles (see Kong et al. 2002b). Also shown in the figures are the optical position of SNRs (*yellow plus signs*) and OB associations (*blue diamonds*). The ellipse shows the D_{25} size of M31. The location of M32 is marked. North is up, and east is to the left.

(Fig. 1, *white dots*), while the larger part of field 2, containing the aim point, is field 2A. There are 12 GC X-ray sources in fields 1, 2A, and 3A + 3B.

For each observation, we examined the background and rejected all high-background intervals. Only events with photon energies in the range of 0.3–7 keV were included in our analysis. The three observations in each field were merged. To detect sources we used CIAO task *wavdetect* (Freeman et al. 2002). Source count rates were determined via aperture photometry and were corrected for effective exposure and vignetting. The radius of the aperture was varied with the average off-axis angle to match the 90% encircled energy function. Background was extracted from an annulus centered on each source. Every extraction region was examined carefully in the images, and in some cases, we had to modify the extraction region to avoid nearby sources. Sources clearly associated with M32 are excluded from this analysis. Obvious foreground stars (see R. Di Stefano et al. 2003, in preparation, for details) were excluded. The total number of sources detected in fields 1, 2, and 3 are 53, 99, and 65, respectively. Detailed source lists and source properties of all the sources in our fields will be presented in forthcoming papers.

3. X-RAY LUMINOSITY FUNCTIONS OF THE X-RAY SOURCES

The background subtracted count rates were converted to luminosities by assuming an absorbed power-law energy spectrum with photon index 1.7, column density $N_{\rm H} = 10^{21}$ cm^{-2} and a distance of 780 kpc. This model is consistent with previous *XMM-Newton* (Shirey et al. 2001) and *Chandra* (Kong et al. 2002b) observations, in which the spectra of many bright point sources could be well fitted by similar models. Although this type of spectral model does not apply to certain classes of sources, such as supersoft sources (R. Di Stefano & A. Kong 2003, in preparation) and supernova remnants (SNRs; e.g., Kong et al. 2002a), the number of such sources in our data sets is small. In general, the luminosities derived by choosing different spectral models (e.g., thermal bremsstrahlung) would differ from the ones we derive by less than a factor of $\sim$2, except for supersoft sources. Considering only power-law spectral models and varying the photon index from 1.2 to 2.5 and sampling values of $N_{\rm H}$ from 7×10^{20} to 5×10^{21} cm^{-2}, we find that our luminosity results can be expressed as $L^{+1.2L}_{-0.2L}$, where L is the luminosity in 0.3–7 keV, and the superscript (subscript) is the maximum (minimum) luminosity associated with any of the models we considered.

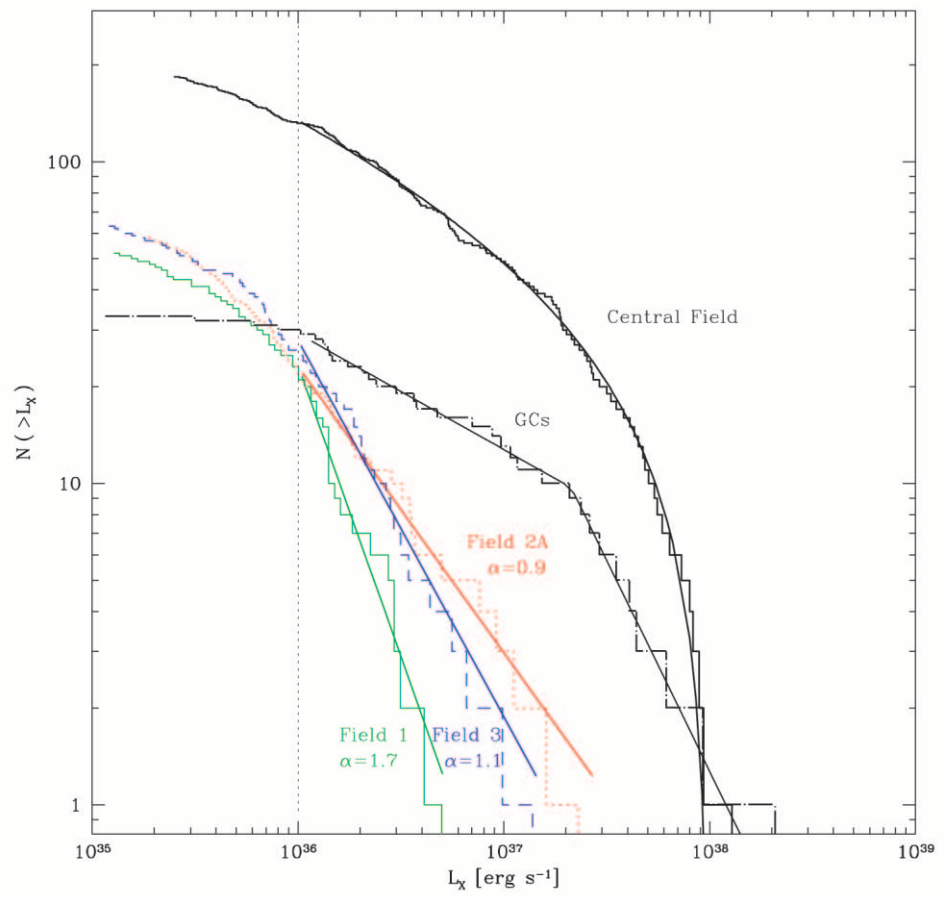

FIG. 2.—Cumulative luminosity functions and their best-fit model for field 1 (*green line*), field 2 (*red line*), field 3 (*blue line*), and globular clusters (*dot-dashed line*). The LF of the bulge (*solid black histogram*) and its best-fit cutoff power-law model (*solid black curve*) are shown for reference. The vertical dotted line represents the completeness limit (10^{36} ergs s^{-1}) of our data.

Figure 2 shows the cumulative LFs for X-ray sources (excluding GCs) in the three fields. Although the detection limit of our observations is about 10^{35} ergs s^{-1}, the LFs flatten below 10^{36} ergs s^{-1}, because the exposure times vary across the images. Following Kong et al. (2002b), we computed histograms of the number of detected sources against the signal-to-noise ratio (S/N) to examine the completeness limit; the histograms peak at S/N $\sim$ 7, corresponding to $\sim 10^{36}$ ergs s^{-1}, and fall off below this. Hence, the LFs are complete down to 10^{36} ergs s^{-1}. Also plotted in Figure 2 are the LFs of X-ray–emitting globular clusters (GCs) and of the bulge region (Kong et al. 2002b).

We used a maximum likelihood method (e.g., Crawford, Jauncey, & Murdoch 1970) to fit the differential LFs with a simple power-law model ($dN/dL \propto L^{-\beta}$). We note that the exponent for a fit to the cumulative LF would be $\alpha = \beta - 1$. The best-fit slopes are shown in Table 1. Field 1 has the steepest slope of $\alpha = 1.7^{+0.34}_{-0.15}$ and normalization of 24 sources at 10^{36} ergs s^{-1}. The slopes of field 2A (the section without the core region) and 3B (the part outside the star-forming ring) are similar; field 2A has a slope of $0.9^{+0.16}_{-0.12}$ and normalization of 24 sources at 10^{36} ergs s^{-1}, while field 3 has a slope of $1.1^{+0.20}_{-0.10}$ and normalization of 27 sources at 10^{36} ergs s^{-1}.

Some of the sources may be background active galactic nuclei (AGNs). We estimated the contribution of background objects by using number counts from the *Chandra* Deep Field Survey (e.g., Brandt et al. 2001; Giacconi et al. 2001). We found that at $\sim 10^{36}$ ergs s^{-1}, about 10 sources in each field should be background objects. We checked this result by counting the numbers of serendipitous point sources in each of several fields from the ChaMP (*Chandra* Multiwavelength Project) archives (P. Green 2002, private communication); in each of five ACIS-S observations of duration comparable to our exposure times, the number of sources with count rates that would correspond to M31 sources with $L_X > 10^{36}$ ergs s^{-1} is less than 10. Therefore, background AGNs and foreground stars have only a modest effect on the LF. By specifically subtracting the effect of the background LF (e.g., Brandt et al. 2001; Giacconi et al. 2001), we found that the uncertainty in the slope due to background effects is within the 1 σ uncertainty limits for field 2A and field 3B. For field 1, the slope steepens when we include background effects, from 1.7 to 3.6, suggesting that the LF of field 1 listed in Table 1 is very likely a lower limit.

4. INTERPRETATION

We have two goals: (1) to relate the X-ray properties of point sources in each group (fields 1, 2, 3, the GCs, and the central region) to properties (such as age) of the underlying stellar population, (2) to understand what the results imply

TABLE 1
LUMINOSITY FUNCTIONS

	Power Law		Cutoff Power Law	
Region	Slope (α)	Break ($\times 10^{37}$ ergs s^{-1})	Slope (α)	Cutoff ($\times 10^{37}$ ergs s^{-1})
Field 1	$1.7^{+0.34}_{-0.15}$	...	...	...
Field 2A	$0.9^{+0.16}_{-0.12}$	...	...	...
Field 3B	$1.1^{+0.20}_{-0.10}$	...	...	...
$r1$[a]	$0.88^{+0.32}_{-0.26}$, $0.73^{+0.15}_{-0.13}$	$\sim$0.2	...	...
$r2$[b]	$0.58^{+0.11}_{-0.10}$, $0.78^{+0.21}_{-0.17}$	$\sim$0.7	...	...
$r3$[c]	0.55 ± 0.06, $1.93^{+0.54}_{-0.47}$	$\sim$2	...	...
$r1 + r2 + r3$	$0.50^{+0.06}_{-0.03}$, $1.58^{+0.28}_{-0.25}$	$\sim$2	0.25 ± 0.07	9.83 ± 0.40
GCs	0.3 ± 0.18, 1.2 ± 0.08	$\sim$2	...	...
Integrated[d]	0.88 ± 0.04, 1.26 ± 0.05	$\sim$2	0.49 ± 0.07	$10.60^{+0.90}_{-0.40}$

NOTE—Uncertainties are 1 σ. The two values in the power-law model are the slope below and above the luminosity break.
[a] Central $2' \times 2'$.
[b] Central $8' \times 8'$ excluding $r1$.
[c] Central $17' \times 17'$ excluding $r1 + r2$.
[d] Includes all sources from the central region ($r1 + r2 + r3$; Kong et al. 2002b) and the disk (fields 1, 2A, and 3).

for X-ray observations of distant galaxies that may be similar to M31.

We begin by counting the number of optically identified OB associations (Magnier et al. 1993), SNRs (d'Odorico et al. 1980; Braun & Walterbos 1993; Magnier et al. 1995), planetary nebulae (PNe; Ford & Jacoby 1978; Ciardullo et al. 1989; R. Ciardullo 2002, private communication) and GCs (Battistini et al. 1987; Magnier 1993; Barmby & Huchra 2001) in each of the three fields. Although these catalogs may not be complete and certainly suffer from a variety of selection effects, they do provide a gross indication of the stellar populations inhabiting each field. Table 2 summarizes the results.

We now propose to study the X-ray properties of each field and relate them to the stellar populations that inhabit the field. Because each field was the subject of identical X-ray observations, comparisons of X-ray properties across fields are well-defined. The situation is not as straightforward for optical observations.

4.1. *Optical Observations*

All of our three fields were surveyed for GCs (Battistini et al. 1987; Magnier 1993; Barmby & Huchra 2001) and PNe (Ford & Jacoby 1978; Ciardullo et al. 1989; R. Ciardullo 2002, private communication). The entire galaxy was also surveyed by *Infrared Space Observatory ISO* far-infrared (175 μm) observations (Schmidtobreick, Haas, & Lemke 2000).

TABLE 2
SOURCE STATISTICS IN THE FIELDS OF VIEW

		Field 2		Field 3	
Source	Field 1	A	B (Nucleus)	A (Young)	B (Old)
$N_{\text{X-ray}}$ (including GCs)	53	68	31[c]	16	49
$N_{\text{X-ray GC}}$	0	11	2[c]	0	1
$N^{\text{opt}}_{\text{GC}}$ (fraction[a])	16 (25.4%)	145 (42%)	57 (27%)	30 (27%)	45 (71%)
$N^{\text{opt}}_{\text{PN}}$ (fraction)	36 (57.1%)	113 (33%)	151 (72%)	18 (16%)	18 (29%)
$N^{\text{opt}}_{\text{SNR}}$ (fraction)	11 (17.5%)	65 (19%)	0 (0%)	48 (42%)	0 (0%)
$N^{\text{opt}}_{\text{OB}}$ (fraction)	0 (0%)	19 (6%)	2 (1%)	17 (15%)	0 (0%)
Average L_{X}[b]	1.14	2.35	13	1.15	1.82
Maximum L_{X}	5	26	60	3.3	420

NOTE—For comparison, there are 12 GC X-ray sources in all fields, while 11 of them are in field 2A. The average and maximum 0.3–7 keV luminosity of GCs is 2.8×10^{37} and 4×10^{38} ergs s^{-1}, respectively; $N_{\text{X-ray}}$ is the total number of X-ray sources; N^{opt} is the number of particular optical sources.
[a] Fraction is defined as the number of this type of optical object divided by the total number of optical sources (GCs + PNe + SNRs + OB associations).
[b] The 0.3–7 keV luminosity (excluding GCs) in units of 10^{36} ergs s^{-1}.
[c] This number is an underestimate because the spatial resolution in this region is significantly degraded (see text).

Data are also available for optically identified OB associations (Magnier et al. 1993) and for SNRs (d'Odorico et al. 1980; Braun & Walterbos 1993; Magnier et al. 1995). Field 2, which is closest to the galaxy center, was fully covered by each of these surveys, but only roughly half of field 1 and $\lesssim 20\%$ of field 3, as described below, were covered.

4.2. *The Fields*

Field 1.—Field 1 is in the far southwestern end of the disk, $\sim 70'$ or 16 kpc from the galactic center. Since all fields received identical X-ray coverage, we can say that the spatial density of X-ray sources in field 1 is lower than in the other fields, the slope of the LF is steeper, and the maximum point-source X-ray luminosity is smaller. In fact, the population is dominated by faint X-ray sources ($<10^{37}$ ergs s^{-1}). The only optical counterparts we found are four possible foreground stars (R. Di Stefano et al. 2003, in preparation). Two far-infrared knots are located in the northeast corner of the field (Schmidtobreick, Haas, & Lemke 2000), which might hint at the presence of a young population in this portion of the field. This is consistent with the presence of a clump of 10 SNRs near the far-infrared knots. These 10 SNRs were discovered by Magnier et al. (1995) in a survey that covered approximately half of field 1. No additional field 1 SNRs were found in that survey, in spite of the fact the area of field 1 that was surveyed was ~ 10 times larger than the region defined by the SNR clump. In addition, no OB associations were found in field 1 (Magnier 1993), although only roughly half of the field was surveyed. One additional SNR was discovered in field 1 (d'Odorico 1980) in a photographic survey. The combination of these data indicate that only a small portion of the northern half of field 1 contains a young stellar population. This implies that roughly half of the field 1 X-ray sources lie in regions not associated with young stellar populations. Apart from the absence of far-infrared knots in the southern portion of field 1, we have no clear indication about the presence or absence of SNRs or OB associations. We therefore refer to the integrated optical light. According to Walterbos & Kennicutt (1988), the total integrated B magnitude is roughly 4 mag dimmer at the location of field 1 than near the galaxy center, and the values of $U-B$, $B-V$, and $B-R$, show that this region is clearly redder than the central region. This trend is supported by other investigations (see Hodge & Kennicutt 1982, and references in Hodge 1992). On the basis of this continuum light, it would be surprising if the southern half of field 1 housed a large young population of stars. We note further that for the total numbers of SNRs and OB associations in field 1 to be comparable to those in fields 2 or 3A, their local density in the southern half of field 1 would have to be even larger than their density in field 2.

Field 2.—Field 2 has the highest spatial density of X-ray point sources. The average and maximum X-ray source luminosities are also highest in field 2. The slope of its LF is significantly smaller than that of field 1 and is similar to slopes measured in starburst galaxies and in the star formation regions of spirals (e.g., Pence et al. 2001; Tennant et al. 2001; Kilgard et al. 2002; Soria & Kong 2002). Field 2 is close to the galaxy center, where the density of GCs is highest; 11 X-ray sources in field 2A (the portion near the aim point) have been identified with GCs (see also Di Stefano et al. 2002). One source in field 2 appears to be coincident with an SNR. Far-infrared observations (Haas et al. 1998; Schmidtobreick et al. 2000) have hinted at star formation activities near the bulge. In particular, there are nine bright far-infrared knots (Schmidtobreick et al. 2000) that are coincident with the X-ray sources in field 2. The density of cataloged optical sources is highest; more than 80 optical sources are SNRs or OB associations, indicating a significant presence of young stars. It therefore seems likely that the X-ray properties of at least a portion of the population in field 2 is characteristic of young stellar populations.

Field 3.—In terms of its distance from the nucleus, the X-ray properties of its point sources, and the numbers and types of optical sources, field 3 lies between fields 1 and 2. The slope of the LF of field 3 is determined almost entirely by sources outside the star-forming ring (field 3B). In fact, the inclusion or exclusion of the sources from field 3A (the section near the star forming ring) does not significantly affect the fit, since only five sources (above 10^{36} ergs s^{-1}) belong to field 3A.

Field 3A was well-covered by the surveys for SNR and OB associations, and visual examination of the optical fields (Magnier et al. 1995) demonstrates that these objects are highly concentrated in the star-forming ring. The region adjacent to the ring was also covered by the surveys. We therefore know that there is a sharp spatial cutoff in the distribution of SNRs and OB associations, with no indication of them away from the ring. There is, therefore, no sign that the regions not surveyed for SNRs and OB associations are rich with these objects. This conclusion is consistent with the distribution of far-infrared knots: there are three such knots, and although the entire field was searched, all three are located along the star-forming ring. The total integrated B magnitude is roughly 3 mag dimmer at the location of field 3 than near the galaxy center (Walterbos & Kennicutt 1988), and as for field 1, the values of $U-B$, $B-V$, and $B-R$, show that the region is redder than the central region (see also Hodge & Kennicutt 1982) It therefore seems unlikely that field 3B houses a large young population.

It is perhaps puzzling that the slope of field 3's LF is essentially the same as for field 2 (within the uncertainty limits), but is less steep than field 1.

GCs.—The LF of GCs differs from that of all three disk fields and the central region. We consider all GC X-ray sources (34 in total) that have been observed by *Chandra*, including both disk (Di Stefano et al. 2002; R. Di Stefano et al. 2003, in preparation) and bulge (Kong et al. 2002b). The power-law model has a break at $\sim 2 \times 10^{37}$ ergs s^{-1}, similar to the central region but the slopes (below and above the break) of the LF are flatter than that of the central region (Kong et al. 2002b). It is worth noting that the luminosity break is also near the luminosity of the brightest GC in our Galaxy (see Di Stefano et al. 2002). The average and maximum luminosity of GCs is also significantly higher than that of fields 1, 2, and 3 (see Table 2 and Fig. 2).

Integrated LF.—To compare M31 with more distant galaxies, it is useful to study the composite M31 LF. This consists of data from both the central region (Kong et al. 2002b) and the disk regions (see Fig. 3). As in the central region of M31 (e.g., Primini, Forman, & Jones 1993; Shirey et al. 2001; Kong et al. 2002b; Kaaret 2002), there is a luminosity break at $\sim 2 \times 10^{37}$ ergs s^{-1}. This break might represent an aging X-ray binary population (Wu 2001; Kilgard et al. 2002; Kaaret 2002). We fit the differential LF with two power-law models with a break at $\sim 2 \times 10^{37}$ ergs s^{-1}, and the results are summarized in Table 1. The shape of the inte-

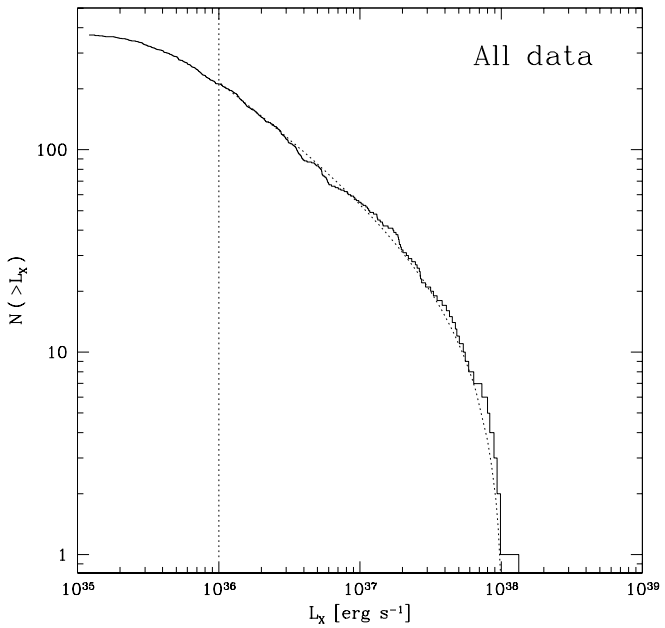

FIG. 3.—Integrated (combining the central $17' \times 17'$ region, fields 1, 2, and 3) cumulative luminosity function of M31. The vertical dotted line represents the completeness limit (10^{36} ergs s^{-1}) of our data. The dotted curve shows the cutoff power-law fit with cutoff luminosity at 10^{38} ergs s^{-1} for the data.

grated LF differs from that of the central region, as fields 1, 2A, and 3 have less luminous sources ($\lesssim 2 \times 10^{37}$ ergs s^{-1}) and have relatively steep slopes for the LF. The slope of the integrated LF below $\sim 2 \times 10^{37}$ ergs s^{-1} is therefore steeper than that of the bulge region (see Table 1). The slope of the integrated LF above the break is consistent with that of GCs, suggesting that luminous X-ray sources of M31 are dominated by GCs.

We also fit the differential LF with a cutoff power-law model ($dN/dL \propto L^{-\beta} e^{-L/L_{\rm cut}}$; Grimm et al. 2002 and Trudolyubov et al. 2002). The best-fitting slope ($\alpha = \beta - 1$) and cutoff luminosity, $L_{\rm cut}$, are 0.49 and 1.06×10^{38} ergs s^{-1}, respectively. Compared to the central $17' \times 17'$ region, the slope is steeper, while the cutoff luminosity is roughly the same (see Table 1). It is worth noting that the cutoff power law fitted to the central $17' \times 17'$ region is in good agreement with the central $15'$ observed with *XMM-Newton* (Trudolyubov et al. 2002). The best-fit parameters of the integrated LF are consistent with the LF of low-mass X-ray binaries (LMXBs) in our own Galaxy (Grimm et al. 2002), which could indicate that LMXBs are important components of M31's X-ray population.

5. CONCLUSIONS

5.1. *Connections between Optical and X-Ray Properties*

With the large number of X-ray sources in each of several different stellar environments, it is appropriate to look for patterns that may relate the LF of each region to its stellar properties. Developing such a relationship could be useful in the study of more distant galaxies in which the X-ray sources and/or the stellar environments are not as well resolved as in M31.

Judging by the numbers and types of optical sources in fields 1, 3, and 2, it seems as if there is a progression from an old population (field 1), to another old population which adjoins a region of star formation (field 3), to the very mixed population near the galaxy center, which includes a significant subpopulation of young stars (field 2). The X-ray properties also seem to exhibit a progression. The slope of the LF is steepest in field 1 and less steep in fields 2 and 3. The density of X-ray sources increases from field 1, to field 3, and is highest in field 2. The value of the maximum source luminosity increases as well.

In spite of these apparent trends, it is wise to be cautious since there are also some apparent discrepancies when we make comparisons with complementary data sets. We first consider ACIS-I observations of the galaxy center, which have also been used to construct LFs (Kong et al. 2002b). The two inner regions, $r1$ and $r2$ encompass $8' \times 8'$ around the galaxy center; together they include 92 point sources. The LFs in these two regions are similar; the composite has slope 0.80 ± 0.13 above the luminosity break (see Kong et al. 2002b). That this is obviously comparable to the slope of field 2A's LF, since 2A and ($r1 + r2$) are close to each other. The puzzle is that $r3$, which covers the central $17' \times 17'$ (excluding $r1 + r2$), and includes 112 point sources, has a markedly different slope, $1.93^{+0.54}_{-0.47}$, much closer to the slope of field 1.

A second relevant comparison can be made with *XMM-Newton* observations of the northern disk (North1 + North2; Fig. 1; Trudolyubov et al. 2002). The LF also has a slope ($\alpha = 1.3 \pm 0.2$) intermediate between that of field 1 and field 3B. Yet, judging by the location of OB associations and SNRs (see Fig. 1), the stellar population would appear likely to have much in common with field 3A and perhaps field 2. Indeed, by comparing with our Galaxy (Grimm et al. 2002), Trudolyubov et al. (2002) concluded that the northern disk of M31 is dominated by faint and young high-mass X-ray binaries (HMXBs). It is worth noting that Grimm et al. (2002) derived a slope of 0.63 ± 0.13 for the cumulative LF of HMXBs in our Galaxy, which is significantly flatter than that of the *XMM-Newton* northern disk fields. In contrast, the LF of field 2A is closer to the Galactic HMXB population (but note that there are uncertainties due to the differences in energy coverage of *Chandra*, *XMM-Newton* and *RXTE*/ASM and other instrumental effects).

These examples make it clear that the slope, taken by itself, is not a good indication of the age of the underlying stellar population, and hence of the age and character of the X-ray sources. Yet, while the slopes of LFs for dissimilar stellar populations may be the same, other qualities (e.g., average and maximum luminosities and source densities) differ, and these combined with information about X-ray colors (Prestwich et al. 2002) may break the degeneracy.

5.2. *GCs*

The data on M31's GCs demonstrate two things. First, there is an important difference between a subset of the X-ray GCs in M31 and the X-ray GCs in the Galaxy. In fact, all of the M31 GC sources above the high-luminosity break are more luminous than any Galactic GC X-ray source; i.e., this part of the M31 GC luminosity function has no Galactic analog. It has been argued on the basis of binary evolution, that these high L_X sources may be a signal that a subset of M31's GCs may be younger than Galactic GCs

(Di Stefano et al. 2002). The possible future evolution of the LF toward lower luminosities may also support this interpretation. Second, if the shape of the LF is a reliable guide, there is an important difference between M31's X-ray sources in GCs and the X-ray sources in both the central field and the disk. If a significant portion of non-GC sources are objects that were once ejected from GCs, it will be necessary to determine how the GC LF can evolve into either the LF of sources in the central field (where most of the GCs reside) or into the LFs found for disk sources.

5.3. *The Integrated Luminosity Function of M31*

The integrated LF makes it clear that observers in distant galaxies would not find M31 to be a very impressive X-ray galaxy. If observers in the Virgo cluster were to observe M31 with the equivalent of a 40 ks ACIS-S observation, only a handful (four) of sources (those with $L_X \gtrsim 10^{38}$ ergs s^{-1}) would be visible at any given time. Half of these would be near the center of the galaxy; the remaining sources would be in GCs. Field 1 would have no detectable sources; field 3A would be, at best, sparsely populated. This result is consistent with earlier surveys (Supper et al. 1997, 2001) and with *XMM-Newton* data (Shirey et al. 2001; Trudolyubov et al. 2002). Although our own Galaxy may house a somewhat larger number of sources with $L_X \lesssim 10^{38}$ ergs s^{-1} (Grimm et al. 2002), the basic result holds for our Galaxy as well, with the difference that it is likely that none of the detectable sources would be in GCs. This result makes it clear that the Galaxy we live in and its nearest neighbor are very different from the distant galaxies on which many current X-ray studies concentrate.

We are grateful to Paul Green and the ChaMP collaboration[2] for providing blank field data and Phil Kaaret for discussions. This work was supported in part by NASA under GO 1-2091X, NAG 5-10889, and NAG 5-10705.

[2] See http://hea-www.harvard.edu/CHAMP.

REFERENCES

Barmby, P., & Huchra, J. P. 2001, AJ, 122, 2458
Battistini, P., Bonoli, F., Braccesi, A. Federici, L., Fusi Pecci F., Marano, B., & Borngen, F. 1987, A&AS, 67, 447
Brandt, W. N., et al. 2001, AJ, 122, 2810
Braun, R., & Walterbos, R. A. M. 1993, A&AS, 98, 327
Ciardullo, R., Jacoby, G. H., Ford, H. C., & Neill, J. D. 1989, ApJ, 339, 53
Crawford, D. F., Jauncey, D. L., & Murdoch, H. S. 1970, ApJ, 162, 405
Di Stefano, R., Kong, A. K. H., Garcia, M. R., Barmby, P., Greiner, J., Murray, S. S., & Primini, F. A. 2002, ApJ, 570, 618
d'Odorico, S., Dopita, M. A., & Benvenuti, P. 1980, A&AS, 40, 67
Ford, H. C. & Jacoby, G. 1978, ApJ, 219, 437
Freeman, P. E., Kashyap, V., Rosner, R., & Lamb, D. Q. 2002, ApJS, 138, 185
Giacconi, R., et al. 2001, ApJ, 551, 624
Grimm, H.-J., Gilfanov, M., & Sunyaev, R. 2002, A&A, 391, 923
Haas, M., Lemke, D., Stickel, M., Hippelein, H., Kunkel, M., Herbstmeier, U., & Mattila, K. 1998, A&A, 338, L33
Hodge, P. 1992, The Andromeda Galaxy (Dordrecht: Kluwer)
Hodge, P., & Kennicutt, R. 1982, AJ, 87, 264
Kaaret, P. 2002, ApJ, 578, 114
Kilgard, R. E., Kaaret, P., Krauss M. I., Prestwich A. H., Raley, M. T., & Zezas, A. 2002, ApJ, 573, 138
Kong, A. K. H., Garcia, M. R., Primini, F. A., & Murray, S. S. 2002a, ApJ, 580, L125
Kong, A. K. H., Garcia, M. R., Primini, F. A., Murray, S. S., Di Stefano, R., & McClintock, J. E. 2002b, ApJ, 577, 738
Macri, L. M., et al. 2001, ApJ, 549, 721
Magnier, E. A. 1993, Ph.D. thesis, MIT
Magnier, E. A., Prins, S., van Paradijs, J., Lewin, W. H. G., Supper, R., Hasinger, G., Pietsch, W., & Truemper, J. 1995, A&AS, 114, 215
Magnier, E. A., et al. 1993, A&A, 278, 36
Pence, W. D., Snowden, S. L., Mukai, K., & Kuntz, K. D. 2001, ApJ, 561, 189
Prestwich, A. H., Irwin, J. A., Kilgard, R. E., Krauss, M. I., Zezas, A., Primini, F. A., Kaaret, P. 2002, ApJ, submitted
Primini, F. A., Forman, W., & Jones, C. 1993, ApJ, 410, 615
Schmidtobreick, L., Haas, M., & Lemke, D. 2000, A&A, 363, 917
Shirey, R., et al. 2001, A&A, 365, L195
Soria, R., & Kong, A. K. H. 2002, ApJ, 572, L33
Stanek, K. Z., & Garnavich, P. M. 1998, ApJ, 503, L131
Supper, R., Hasinger, G., Lewin, W. H. G., Magnier, E. A., van Paradijs, J., Pietsch, W., Read, A. M., & Trumper, J. 2001, A&A, 373, 63
Supper, R., Hasinger, G., Pietsch, W., Trumper, J., Jain, A., Magnier, E. A., Lewin, W. H. G., & van Paradijs, J. 1997, A&A, 317, 328
Tennant, A. F., Wu, K., Ghosh, K. K., Kolodziejczak, J. J., & Swartz, D. A. 2001, ApJ, 549, L43
Trinchieri, G., & Fabbiano, G. 1991, ApJ, 382, 82
Trudolyubov, S. P., Borozdin, K. N., Priedhorsky, W. C., Mason, K. O., & Cordova, F. A. 2002, ApJ, 571, L17
Walterbos, R., & Kennicutt, R. 1988, A&A, 198, 61
Wu, K. 2001, Publ. Astron. Soc. Australia, 18, 443